

Public Domain Mark 1.0 Universal

This work was written as part of one of the author's official duties as an Employee of the United States Government and is therefore a work of the United States Government. In accordance with 17 U.S.C. 105, no copyright protection is available for such works under U.S. Law.

Access to this work was provided by the University of Maryland, Baltimore County (UMBC) ScholarWorks@UMBC digital repository on the Maryland Shared Open Access (MD-SOAR) platform.

Please provide feedback

Please support the ScholarWorks@UMBC repository by emailing scholarworks-group@umbc.edu and telling us what having access to this work means to you and why it's important to you. Thank you.

A MODIS-derived photochemical reflectance index to detect inter-annual variations in the photosynthetic light-use efficiency of a boreal deciduous forest

Guillaume G. Drolet^a, Karl F. Huemmrich^{b,c}, Forrest G. Hall^{b,c}, Elizabeth M. Middleton^b,
T. Andrew Black^d, Alan G. Barr^e, Hank A. Margolis^{a,b,*}

^a Faculté de Foresterie et de Géomatique, Pavillon Abitibi-Price, Université Laval, Sainte-Foy, Québec, Canada G1K 7P4

^b Biospheric Sciences Branch, Code 614.4, NASA/Goddard Space Flight Center, Greenbelt, Maryland 20771, USA

^c Joint Center for Earth Systems Technology, University of Maryland, Baltimore County, Baltimore, Maryland 21228, USA

^d Faculty of Agricultural Sciences, 135-2357 Main Mall, University of British Columbia Vancouver, British Columbia, Canada V6T 1Z4

^e Climate Research Branch, Meteorological Service of Canada, 11 Innovation Blvd. Saskatoon, Saskatchewan, Canada S7N 3H5

Received 14 May 2005; received in revised form 8 July 2005; accepted 9 July 2005

Abstract

The relationships between ecosystem-level light use efficiency (LUE) obtained from an eddy covariance flux tower and MODIS-derived values of a scaled Photochemical Reflectance Index (sPRI) were investigated for a boreal aspen stand (*Populus tremuloides* Michx.) in Saskatchewan, Canada. Using MODIS ocean band 11 at 531 nm, we tried to detect variations in canopy reflectance related to the xanthophyll cycle. We tested several other MODIS bands as the reference band because the 570 nm reference band that had been determined to be optimum for calculating PRI in earlier studies is not available on MODIS.

While LUE varied greatly within the 2001, 2002, and 2003 growing seasons, the Normalized Difference Vegetation Index (NDVI) calculated from tower sensors remained stable. LUE had a negative exponential relationship with vapor pressure deficit and air temperature, and was at a maximum when absorbed PAR was $<200 \mu\text{mol m}^{-2} \text{s}^{-1}$. The range and magnitude of tower-based LUE values were smaller on clear days, when MODIS acquisitions were possible, than they were overall. Furthermore, the orbital parameters of the Terra and Aqua satellites restricted MODIS acquisitions to a 2.5-h period in early afternoon at our study site when LUE values were typically lower than they were earlier in the day.

Strong correlations between MODIS-sPRI and LUE were found only for backscatter reflectance scenes when band 13 (667 nm) was used as the reference band. The correlations were higher for sPRI calculated from top of atmosphere reflectances than for surface reflectances ($r^2=0.76$ and 0.53 , respectively). The absolute backscatter reflectance of bands 11, 12 (551 nm), and 13 all decreased with increasing LUE. The decrease in band 13 suggests that the correlation between sPRI and LUE that we observed was caused by reductions in canopy chlorophyll content from 2001 to 2003 and/or by increased visibility of brighter non-photosynthetic material. Regional values of sPRI from 260 deciduous forest pixels in the 10,000 km² vicinity of the tower for two contrasting days, one in 2001 and one in 2003, were consistent with that observed for the flux tower footprint.

© 2005 Elsevier Inc. All rights reserved.

Keywords: Photochemical reflectance index; MODIS; Light use efficiency; Gross primary production; Boreal deciduous forest; Regional analysis

1. Introduction

Between 90 and 130 Tg of carbon (C) are absorbed annually from the atmosphere by terrestrial ecosystems through the physiological process of photosynthesis (Cramer et al., 2001). This photosynthetic flux, referred to

* Corresponding author. Faculté de Foresterie et de Géomatique, Pavillon Abitibi-Price, Université Laval, Sainte-Foy, Québec, Canada G1K 7P4. Tel.: +1 418 656 7120; fax: +1 418 656 5262.

E-mail address: Hank.Margolis@sbf.ulaval.ca (H.A. Margolis).

as gross primary productivity (GPP), is one of the largest components of the global C cycle (Bolin & Fung, 1992). Within the C cycle, autotrophic (R_a) and heterotrophic (R_h) respiration return C to the atmosphere. All these elements of the C cycle are sensitive to climate variability (e.g., Amiro et al., in press; Barr et al., 2004), and they tend to interact in complex ways with environmental factors such as light, nutrients, soil water, vapor pressure deficit, air temperature, and soil temperature.

As one of the largest biomes in the world, the boreal forest plays a key role in the global C cycle (Hall et al., 2004; Schlesinger, 1997). CO_2 -induced climate change may be occurring at boreal latitudes (Kattenberg et al., 1996; Mitchell et al., 1990), leading to longer growing seasons or more intense droughts. Such climate perturbations could in turn affect the spatial and temporal characteristics of the terrestrial C cycle in boreal forests. Since the net annual C flux can be close to zero for mature forest stands (Amiro et al., in press; Goulden et al., 1997, 1998), relatively small changes in climate could influence the direction of the net annual flux. To obtain both reliable current estimates and accurate future predictions of C cycling at larger spatial scales for boreal forests, we need to make the best possible use of remote sensing inputs into ecosystem process models (Running et al., 1999; Turner et al., 2004).

Data from the satellite-borne MODerate Resolution Imaging Spectroradiometer (MODIS) are currently used in the calculation of global weekly GPP at 1-km spatial resolution (Heinsch et al., 2003; Running et al., 2000, 2004). GPP estimates are derived from a light-use efficiency model as elaborated by Monteith (1972, 1977). In this model, net or gross photosynthesis is represented as the product of absorbed photosynthetically active radiation (APAR) and a LUE term. In the MODIS-GPP algorithm, APAR is the product of the fraction of incident photosynthetically active radiation (PAR) absorbed by vegetation (f_{APAR}) derived from MODIS spectral data (Myneni et al., 2002) and the incident PAR, estimated from incident shortwave radiation data from a General Circulation Model (GCM) (Heinsch et al., 2003). LUE is a biome-specific value representing optimal potential (i.e. under non-limiting conditions) of the vegetation for converting PAR to GPP. It is extracted from a look-up table and down-scaled to take into account the restraining effects on LUE of climatic variables (air temperature and vapour pressure deficit) from the GCM dataset. The inaccuracies inherent to this way of estimating LUE can account for much of the differences observed between satellite-based productivity estimates and field measurements (Martel et al., 2005; Running et al., 1999; Turner et al., 2003a). Several other authors have also proposed that LUE values used in ecosystem productivity algorithms do not adequately capture the spatial and temporal variability present across a region (Goetz & Prince, 1996, 1998; Turner et al., 2003b). Clearly, direct measurements of LUE from remote sensing data could

improve estimates of C fluxes from terrestrial ecosystems at regional and global scales.

The photochemical reflectance index (PRI) was developed as a remotely-sensed indicator of LUE (Gamon et al., 1990, 1992). It uses narrow spectral bands to detect changes in leaf reflectance at 531 nm relative to a reference band that is usually located at around 570 nm and is not supposed to be affected by changes in short-term stress events. This change in the reflectance at 531 nm is created by the conversion of the xanthophyll cycle pigment violaxanthin to the de-epoxidized antheraxanthin and zeaxanthin as a way of dissipating excess light to protect the photosynthetic apparatus (Demmig-Adams & Adams, 1996; Demmig-Adams et al., 1998; Holt et al., 2005; Yamamoto, 1979). PRI has been correlated with both the epoxidation state of the xanthophyll cycle pigments and LUE in several field studies at the leaf and ecosystem levels (Gamon et al., 1992, 1997; Peñuelas et al., 1995, 1997; Trotter et al., 2002). Narrow-band spectral reflectance may also provide information on the ratio of carotenoids to chlorophyll a for detecting longer term stress effects and on total chlorophyll concentration for detecting plant nutrient status (Filella et al., 2004).

Eddy covariance (EC) flux towers are the most direct means of estimating LUE of terrestrial ecosystems. Correlations between PRI and ecosystem LUE were recently found when PRI was obtained from hyperspectral data acquired by aircraft (Rahman et al., 2001) and by helicopter-mounted sensors (Nichol et al., 2000). More recently, Rahman et al. (2004) used MODIS reflectance data from bands originally intended for ocean observations and calculated PRI over a temperate deciduous forest. They found a high correlation of MODIS-PRI with daily NPP that was derived from EC data. Given the major role boreal forests play in the global C cycle, it is important to analyze the extent to which MODIS-PRI is capable of estimating LUE in boreal ecosystems. To begin this effort, we selected a boreal aspen stand (*Populus tremuloides* Michx.) in Saskatchewan for which multi-year C flux data were available (Barr et al., 2004). Using flux and meteorological data from this aspen stand, the objectives of the current study were to determine (1) whether MODIS-PRI could track diurnal, day-to-day, seasonal, and/or annual variations in LUE; (2) the influence of view geometry on the PRI–LUE relationship; (3) the relative contribution of each PRI reflectance band to the overall signal; and (4) whether consistent PRI patterns were observable at a regional scale.

2. Methods

2.1. Study site

The study site is located in a mature trembling aspen (*Populus tremuloides* Michx.) forest within Prince Albert

National Park (53.629° N, 106.198° W), Saskatchewan, Canada (Fig. 1). Referred to as the Old Aspen (OA) site, this 70-year old forest was one of several EC flux tower sites that were operated between 1993 and 1996 as part of the Boreal Ecosystem-Atmosphere Study (BOREAS) (Sellers et al., 1995, 1997) and subsequently in the Boreal Ecosystem Research and Monitoring Study (BERMS) (<http://berms.ccrp.ec.gc.ca>). Currently, the site is part of the Fluxnet-Canada Research Network (<http://www.fluxnet-canada.ca>). The ecological characteristics of the Old Aspen site are described in detail by Barr et al. (2004) and Hogg et al. (1997, 2005). It was chosen for the current research effort for two reasons: (a) its homogeneous and dense canopy structure with at least 3 km of fetch in all directions that we believed would minimize undesirable effects on satellite-derived canopy reflectances (e.g., shadow, view and sun angles, background effects, adjacency effects) and (b) the availability of high-quality, multi-year EC flux and meteorological data. For our individual site analyses, data for an area of $\sim 1 \text{ km}^2$ around the EC flux tower was used. This area corresponds approximately to the geometric instantaneous-field-of-view (GIFOV) of an at-nadir MODIS pixel (Barnes et al., 1998) and encompasses the tower footprint area for typical daytime conditions at this site (Blanken et al., 2001).

2.2. Acquisition and processing of MODIS data

The MOD09 daily surface reflectance product could not be used because it does not contain the narrow bands that are of interest for the calculation of PRI, i.e., it uses bands 1 through 7 but does not include bands 11 through 13. Thus, we had to develop a new processing procedure for the MODIS data.

Using measurements of the photosynthetic photon flux density (PPFD) from above-canopy tower sensors (model

LI-190, LI-COR, Lincoln, NE), predominantly clear days were identified for three growing seasons (2001 through 2003). Growing seasons for the current study were defined as days of year (DOY) 152 to 243 (June 1 to August 31), which is a period when the canopy is fully developed (Barr et al., 2004) and the Normalized Difference Vegetation Index (NDVI) time series derived from tower radiometric data stays very stable (e.g., coefficient of variation $< 1.5\%$). For clear days only, four MODIS products from both the Terra (MOD) and Aqua (MYD) satellite platforms were downloaded from the EOS Data Gateway (<http://redhook.gsfc.nasa.gov>). For each scene, the four products were for the same land area (one granule of $1354 \times 2330 \text{ km}$) and included the study site. The first product, MOD/MYD021KM, contained the at-aperture calibrated radiances for the 36 MODIS spectral bands at a spatial resolution of 1 km and included coefficients for calculating the top-of-atmosphere reflectance values. The MOD/MYD03 product consisted of the geolocation and sensor/solar geometry for every pixel in the granule. The third product (MOD/MYD04) contained the aerosol optical thicknesses (AOT) at 550 nm over land at a spatial resolution of 10 km. These AOT values were used for correcting the top-of-atmosphere reflectance data to surface reflectance with the 6S model (Vermote et al., 1997). Finally, the MOD/MYD35 product had a cloud mask used for screening cloud-contaminated pixels.

For each of the selected scenes, the pixel that was closest to the tower (subsequently referred to as the “tower pixel”) was identified using latitudes and longitudes from the MOD/MYD03 product and the tower coordinates. Reflectance values for the tower pixels were then calculated for bands 1, 2, 4, 11, 12 and 13-low gain and extracted along with sensor/sun geometry, pixel geolocation, cloud mask, and AOT. Using the cloud mask information, all the extracted pixels with a cloud mask value other than ‘confident clear’ were excluded from the dataset. Based on visual analyses, we found that the cloud mask often failed to detect cloud-contaminated pixels. For this reason, all the scenes that remained after the screening were inspected visually for possibly undetected cloud contamination. To achieve this, all the acquired scenes were subsetting to a smaller region ($\sim 74,000 \text{ km}^2$) encompassing the study site and geometrically rectified to a linear projection using the HDFLook-MODIS software (http://www-loa.univ-lille1.fr/Hdflook/hdflook_gb.html) to obtain equal-area pixels so that the images could be used in a geographic information system. Only scenes with no clouds in the area surrounding the tower location were kept for further analysis. Finally, all remaining scenes with a sensor zenith angle greater than 40° were rejected to eliminate pixels with a reduced spatial resolution, i.e., with radiances measured over areas much larger than 1 km^2 (Table 1).

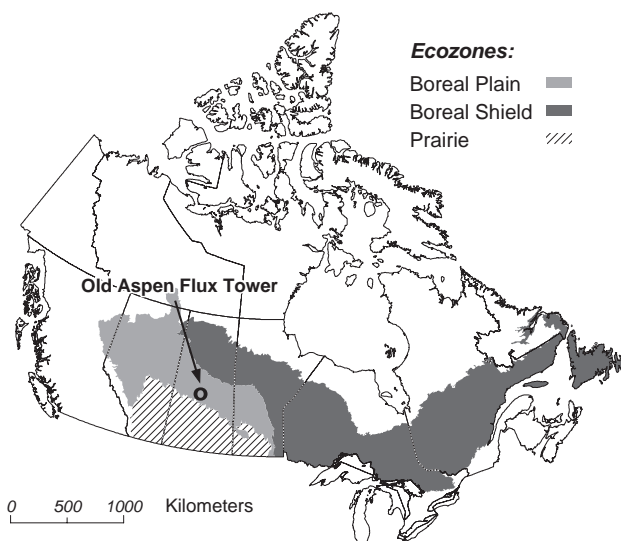


Fig. 1. Location of the study site in Canada.

Table 1
Cloud-free MODIS scenes used in this study

Year	Day	Time (UTC)	Platform	Relative azimuth (°)	Relative zenith (°)
2001	155	1805	T	55.5	3.8
	156	1845	T	114.6	2.9
	185	1815	T	55.2	18.5
	187	1805	T	51.7	3.9
	194	1810	T	54.0	12.2
	201	1815	T	53.3	21.5
	217	1815	T	54.8	25.5
	222	1835	T	119.0	25.6
	228	1755	T	55.4	7.0
	233	1815	T	58.0	30.1
	236	1845	T	115.3	14.4
2002	156	1810	T	54.3	19.0
	166	1845	T	116.7	3.9
	177	1825	T	121.5	18.9
	188	1955	A	42.9	30.6
	190	1755	T	50.0	4.8
	192	1930	A	116.9	1.1
	197	1805	T	50.8	13.0
		1945	A	122.7	26.1
	200	2020	A	53.2	1.6
	201	1925	A	115.5	3.6
	204	1810	T	51.1	22.0
	206	1755	T	50.2	7.5
		1940	A	119.3	19.3
	216	1835	T	120.4	16.8
	236	1810	T	56.6	30.4
		1950	A	58.1	42.6
	239	2025	A	55.4	6.9
	240	1930	A	117.7	13.7
	241	1825	T	119.2	32.8
2003		2010	A	55.8	20.1
	155	1830	T	118.8	11.0
	166	1955	A	53.4	21.1
	169	1845	T	118.2	4.1
	193	1755	T	48.6	4.7
		1940	A	118.7	17.4
	198	1955	A	56.7	22.6
	205	2005	A	54.9	16.1
	208	1850	T	118.7	5.0
	214	1810	T	56.4	31.5
		1955	A	58.6	26.5
	217	1845	T	118.9	3.3
	225	1940	A	118.6	23.8
	226	1835	T	119.3	12.7
		2020	A	55.1	2.2
	227	1925	A	115.9	9.4
	230	1815	T	55.5	36.0
		1955	A	60.1	31.2
	237	1820	T	117.0	41.1
		2005	A	58.2	25.3
	241	1755	T	56.5	16.2

T = Terra, A = Aqua. Numbers of cloud-free MODIS acquisitions were 11, 20, and 20 for 2001, 2002, and 2003, respectively. Total number of cloud-free MODIS acquisitions for the three years is 51.

2.3. Photochemical Reflectance Index (PRI)

For the tower pixels in the dataset that were determined to be cloud-free, PRI was calculated using MODIS band 11 (526–536 nm) as the band containing the PRI signal

since this narrow band is centered at 531 nm (Fig. 2). We tested MODIS bands 1 (620–670 nm), 4 (545–565 nm), 12 (546–556 nm) and 13 (662–672 nm) as potential reference bands. PRI was calculated as:

$$\text{PRI} = (\rho_{11} - \rho_{\text{ref}}) / (\rho_{11} + \rho_{\text{ref}}), \quad (1)$$

where ρ_{11} is MODIS reflectance at 531 nm and ρ_{ref} is a reference band. In addition, to obtain only positive values, PRI was scaled using the mathematical transformation (Rahman et al., 2004):

$$\text{sPRI} = (\text{PRI} + 1) / 2. \quad (2)$$

2.4. Micrometeorological data

Micrometeorological data for the site were downloaded from the FCRN Data Information System (<http://fluxnet-canada.ccrp.ec.gc.ca>) for the growing seasons of 2001 to 2003. The dataset consisted of continuous half-hour averages of gross ecosystem productivity (GEP) derived from EC measurements of net ecosystem exchange (NEE) (Baldocchi, 2003; Baldocchi et al., 1988). GEP is calculated as the net ecosystem productivity (NEP), derived from the NEE measurements ($\text{NEP} = -\text{NEE}$), plus ecosystem respiration (R_{eco}), which is modeled using a relationship between nighttime respiration and soil temperature at 2 cm below the ground surface (Barr et al., 2003; Goulden et al., 1997). GEP is equivalent to GPP as used in the MODIS algorithm. We use the term GEP instead of GPP because GEP is the terminology that is generally used in C flux studies.

Meteorological variables likely to have an impact on LUE were downloaded (e.g., incoming shortwave radiation, PPFD, air temperature, and relative humidity above the canopy) for further analysis of the relationships between environmental stressors, photosynthetic LUE, and PRI. As well, some of these variables were used for calculating f_{APAR} as described below. The methods and instruments

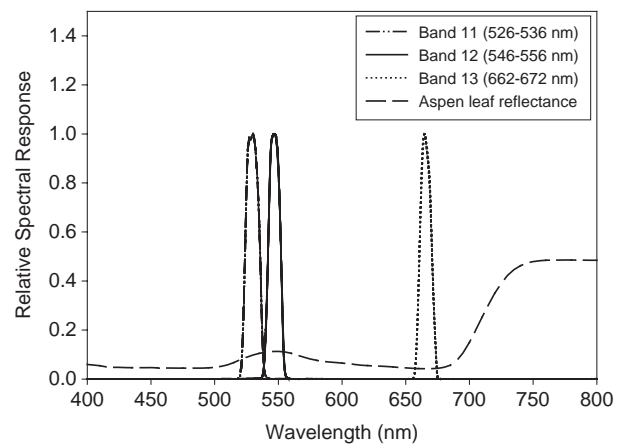


Fig. 2. Relative spectral responses for MODIS-Terra bands 11, 12 and 13-lo (<ftp://ftp.mcst.ssai.biz>). The spectrum for an aspen leaf is also shown (dashed line from 400 to 800 nm) (Middleton & Sullivan, 2000).

used to measure fluxes and meteorological variables at the Old Aspen site are described in Barr et al. (2004) and Blanken et al. (1997).

2.5. Photosynthetic light-use efficiency

For the current study, LUE (in units of $\mu\text{mol CO}_2 \mu\text{mol}^{-1}$ photons of absorbed PAR) of the canopy for the period of a given MODIS acquisition of a tower pixel was calculated as GEP divided by APAR. For every tower pixel used, GEP was extracted for the 30-min period that contained the MODIS acquisition time. The 30-min estimates of GEP were considered to be representative of the LUE at the time of the MODIS overpass for several reasons. The 30-min flux data were quality checked for stationarity, so if the variation between the six 5-min fluxes within a half-hour exceeded a certain threshold, the data for that half-hour were rejected. Large variations in environmental conditions and fluxes were not likely during 30-min periods on the clear days used in this study. Also, the site was very uniform in all directions around the tower, this was why it was originally selected as a BOREAS site. Thus, changes in wind direction did not have a significant impact.

Assuming a relationship between NDVI and f_{APAR} and noting that the tNDVI was very stable between DOY 152 and DOY 243 in the current study, there was essentially no difference in the seasonal pattern of LUE based on incident PAR versus APAR. Nevertheless, we prefer expressing LUE on the basis of APAR since this is what is used for MODIS-based modelling of global and regional photosynthesis (Heinsch et al., 2003; Martel et al., 2005). For each acquisition, NDVI was calculated using PAR (400–700 nm) and total shortwave radiation (285–2800 nm) data from the tower sensors as described in Huemmrich et al. (1999) where optical infrared reflectance (shortwave minus PAR) is used instead of near-infrared. This instantaneous “tower-NDVI” (tNDVI) was then used to derive the instantaneous f_{APAR} as described below. During BOREAS, Chen and Cihlar (1998) measured an average daily green f_{APAR} of 0.79 during the summer at the Old Aspen site using the TRAC sensor (Chen & Cihlar, 1995). The ground-measured LAI in 1994 was 5.16, very close to the total LAI of 5.22 measured in 2001. Thus, we could safely assume that the average green f_{APAR} in 2001 was the same value as in 1994 and that this f_{APAR} value corresponded to the maximum summer tNDVI. With LAI values of 3.99 and 4.03, respectively, in 2002 and 2003, changes in f_{APAR} were small during the study period since f_{APAR} is insensitive to changes in LAI when LAI > 3 in homogenous canopies. We assumed that the green f_{APAR} equals zero at the tNDVI value for the days just before green-up and following the snow melt. We then used linear regression on these two points to calculate the relationship between f_{APAR} and tNDVI (Eq. (3)). For each year, a mean growing season tNDVI was calculated using tower NDVI values for the time of the MODIS overpasses. This mean tNDVI was then used to

derive the growing season f_{APAR} used to calculate the APAR value for each tower pixel (Eq. (4)), by multiplying it by the mean 30-min incident PAR flux for the same period:

$$f_{\text{APAR}} = (1.95 \times \text{tNDVI}) - 0.96 \quad (3)$$

and

$$\text{APAR} = f_{\text{APAR}}(\text{PAR}). \quad (4)$$

2.6. Relationship between sPRI and LUE

The relationship between MODIS-sPRI and tower LUE was analyzed using linear regression (SAS Institute, 2000). The data were verified for homogeneity of variance and an unbiased distribution of residuals. No data transformations were necessary.

2.7. Regional sPRI analysis

Precipitation records show that 2001 was the beginning of a prolonged drought that lasted through 2003 (Hogg et al., 2005). For these two years, two MODIS images (July 6, 2001 and August 14, 2003) were chosen from the regression analysis dataset (backscatter) for a comparison of the sPRI values at the regional scale. Using a 1994 Landsat-5 TM land cover image (Hall & Knapp, 1999), a 9904 km² area was defined around the OA site. Inside this area, 260 cloud-free MODIS pixels with a deciduous cover higher than 65% were extracted in ArcGIS (ESRI, www.esri.com) and ENVI environments (Research Systems Inc., www.rsinc.com). Since extensive patches of deciduous pixels were relatively infrequent inside the designated area, deciduous and medium-age deciduous regeneration classes were aggregated into one class. Finally, reflectance data for both years were atmospherically corrected using AOT from MODIS and the 6S model and mean sPRIs and frequency distribution histograms were calculated and compared using a paired *t*-test.

3. Results

3.1. NDVI and LUE

Time-series of tNDVI at noon local time (LT) for the years 2001 to 2003 show that once the canopy was fully leafed (around day 160 for the three years), tNDVI was quite stable throughout the growing season, with small day-to-day variations (Fig. 3). However, tNDVI in 2003 tended to be lower than it was in 2001 and 2002. The noise in the tNDVI data (line plot) was caused by clouds and it disappeared when only clear days were plotted (symbols) (Huemmrich et al., 1999). This relative stability of tNDVI during the growing season, and thus of f_{APAR} , suggests an inadequacy of the tNDVI to track variations in LUE that

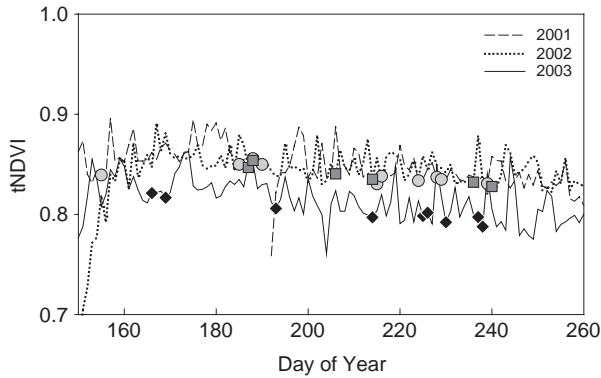


Fig. 3. Seasonal and inter-annual pattern of tower-NDVI (tNDVI) at noon local time as measured by the tower sensors between June and August. Line plots include cloudy and clear days, while symbols show only tNDVI values for clear days with good radiation data at noon (LT), where circles are for 2001, squares for 2002, and diamonds for 2003.

occur at short time scales (e.g., hourly, daily, weekly). For the same time of the day (noon LT), LUE was more dynamic, in response to short-term variations in environmental variables (Fig. 4). Coefficients of variation were 1.0%, 1.2%, and 1.4% for NDVI data on clear days in 2001, 2002, and 2003, versus 77.1%, 90.5%, and 83.3% for LUE. For the days when cloud-free MODIS images were obtained for the site, tower data showed low LUE values.

3.2. Environmental factors and LUE

Half-hourly means of LUE between 9:00 and 15:00 LT, which correspond to an extended period encompassing the

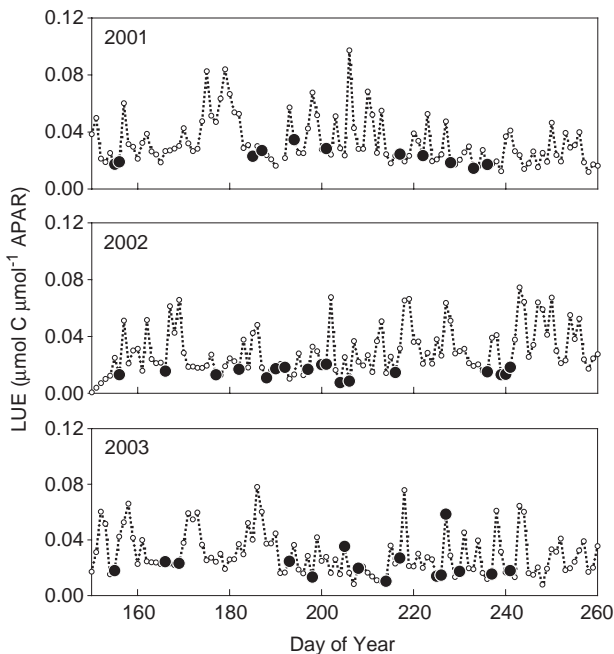


Fig. 4. LUE derived from the tower data at noon local time (open circles) for the growing seasons (June to August) of 2001 to 2003. The black circles show the days with clear MODIS images over the study site.

time period of the acquired MODIS overpasses for June through August 2003, showed that LUE was related to vapor pressure deficit (VPD) and to air temperature above the canopy (Fig. 5a–b). Both figures show negative exponential relationships between LUE and the two environmental variables. Fig. 5c shows that the relationship between GEP and APAR was not linear. Below about $100 \mu\text{mol m}^{-2}\text{s}^{-1}$ APAR, the slope of the relationship (i.e. LUE) was at its maximum. For APAR values greater than $200 \mu\text{mol m}^{-2}\text{s}^{-1}$, GEP was highly variable for a given level of APAR, probably reflecting the effects of environmental factors such as VPD and soil moisture content on the canopy LUE.

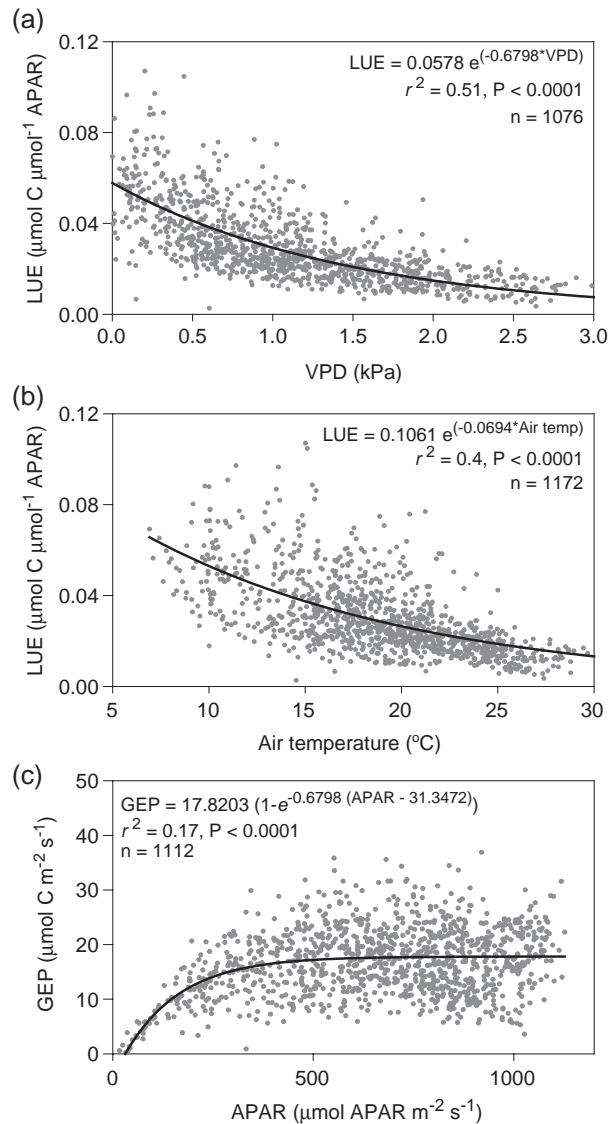


Fig. 5. (a) LUE versus vapor pressure deficit (VPD), (b) LUE versus air temperature above the canopy, and (c) GEP versus the amount of PAR absorbed by the canopy, for the half-hour periods between 9 AM and 3 PM local time, for the months of June through August 2003 at the study site. In (c), LUE is the slope of the relationship between GEP and APAR. The slope reaches a maximum between 0 and around $100 \mu\text{mol m}^{-2}\text{s}^{-1}$ of photons absorbed, after which it starts to decrease.

3.3. Relationship between sPRI and LUE

With band 13 as the reference band, sPRI showed a larger range when MODIS acquisitions from all three years were plotted against LUE for both atmospherically corrected and uncorrected datasets (Fig. 6a) than it did with band 12 as the reference band (Fig. 6b). However, sPRI calculated with band 13 as the reference band did not show a relationship with LUE when all the cloud-free MODIS scenes were included ($r^2=0.05$, $P<0.09$, and $r^2=0.08$, $P<0.04$, for top-of-atmosphere and surface reflectance data, respectively). Although band 12 is the MODIS band that is closest to the reference band used in several other PRI studies (e.g., Nichol et al., 2000; Peñuelas et al., 1995; Rahman et al., 2001), the use of this reference band in the current study showed a very narrow range in sPRI and no relationship with LUE (Fig. 6b) when either backscatter or forward scatter reflectances were used ($r^2=0.002$, $P<0.77$, and $r^2=0.07$, $P<0.06$, for top-of-atmosphere and surface reflectance data, respectively). Using bands 1 and 4 as reference bands gave similar results as band 12, although band 1 showed a larger range in sPRI than band 4 (not shown). In all cases, the relationship between sPRI and LUE was nearly non-existent when data from all MODIS images (i.e. all sun/sensor geometry) were used.

The dataset was subsequently separated into backscatter and forward scatter reflectances. For a given scene, backscatter reflectance (i.e., looking away from the sun with little or no shadows in the field of view) was defined as acquisitions where the relative azimuth angle (difference between sensor and solar azimuth angles) was less than or equal to 60° , and the relative zenith angle (difference between sensor and solar zenith angles) was less than or equal to 10° . Forward scatter pixels (looking into the sun and increased shadowing) were those which had a relative

zenith angle less than or equal to 10° , but with a relative azimuth angle (difference between the sensor and solar azimuth angles) greater than 60° . With these constraints, nine scenes from 2001 to 2003 were found to have backscatter reflectance and nine had forward scatter reflectance. Again, bands 1, 4, 12 and 13 were tested as reference bands and sPRIs were plotted against LUE.

For backscatter data, sPRI calculated with band 13 showed a strong positive linear relationship with LUE for backscatter top-of-atmosphere reflectance ($r^2=0.76$, $P<0.002$) and a weaker relationship when using backscatter surface reflectance ($r^2=0.53$, $P<0.03$) (Fig. 7b). No relationship was found between sPRI (using band 13 as the reference band) and LUE when forward scatter data were used (Fig. 7a). With band 12 as the reference band, a relationship between LUE and sPRI was found for backscatter top-of-atmosphere reflectance data ($r^2=0.52$, $P<0.03$) that was not evident when surface reflectances were used ($r^2=0.15$, $P<0.3$) (not shown). For the remaining reference bands tested, no significant relationships were found between sPRI and LUE when separating backscatter from forward scatter reflectance.

An analysis of the change in absolute backscatter reflectance in bands 11, 12, and 13, relative to the change in LUE for the years 2001 to 2003 showed that the reflectance in the three bands decreased with increasing levels of LUE (Fig. 8). Although there were no significant differences between the slopes of the three relationships, the sPRI data (Fig. 7) suggest that LUE had a slightly stronger effect on the reflectance in band 13 compared to reflectances in bands 11 and 12. It should also be noted that the reflectance in band 11, although expected to increase with increasing levels of LUE according to PRI theory (Gamon et al., 1992), showed the same decreasing trend as bands 12 and 13.

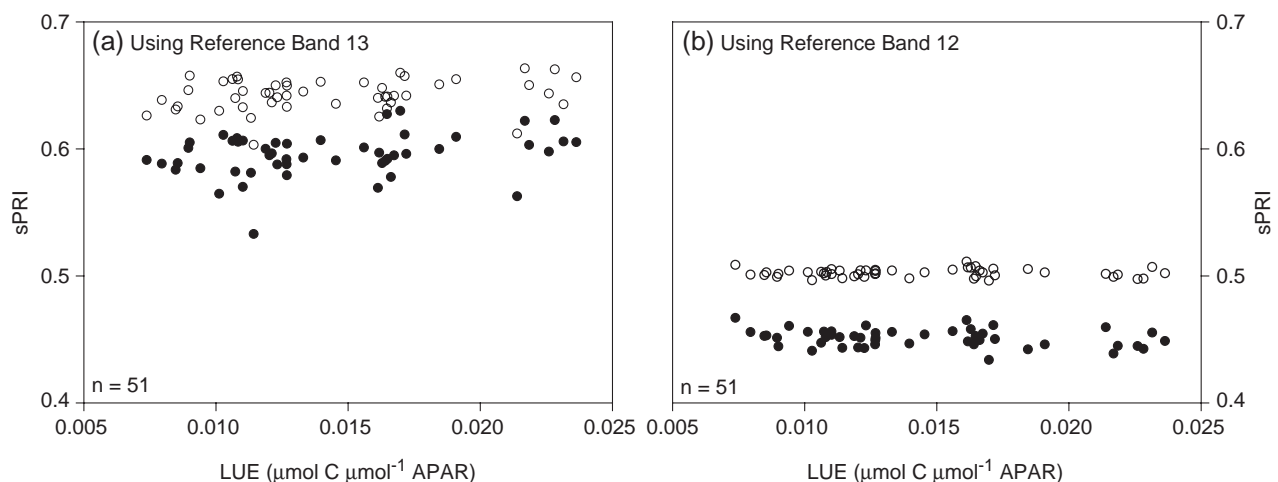


Fig. 6. sPRI versus LUE derived from MODIS reflectance data using all data from band 11 (531 nm) in combination with either (a) band 13 or (b) band 12 as reference bands, for clear days of 2001 to 2003 growing seasons. Open (○) and solid (●) circles indicate top-of-atmosphere and surface reflectance, respectively.

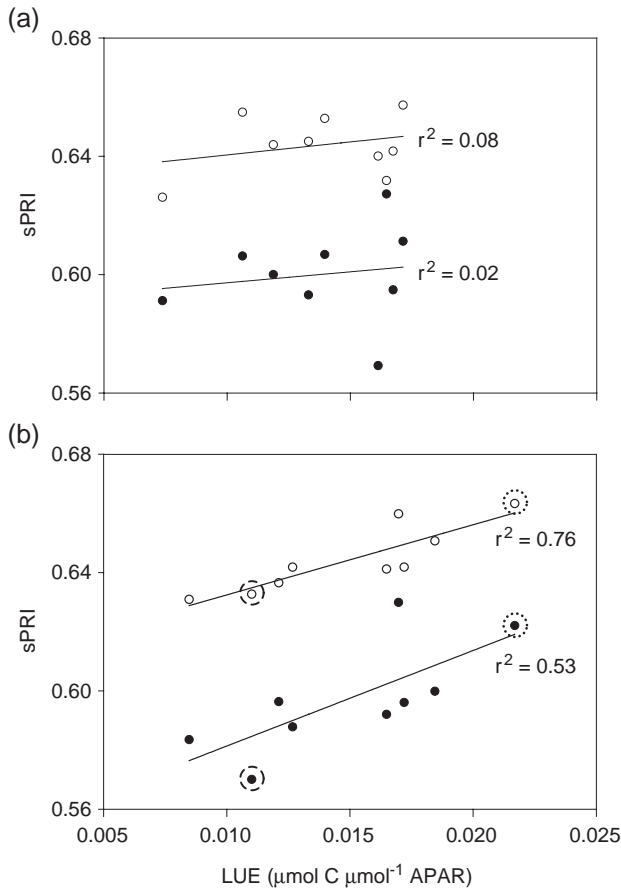


Fig. 7. sPRI versus LUE determined from surface and top-of-atmosphere MODIS reflectance values in bands 11 and 13 for (a) forward scatter and (b) backscatter data for the 2001, 2002, and 2003 growing seasons. Open (○) and solid (●) circles indicate top-of-atmosphere and surface reflectance, respectively. Dotted and dashed circles indicate July 6, 2001 and August 14, 2003, respectively. These two dates were selected for the regional analysis.

3.4. Regional inter-annual comparison of sPRI

The comparison between mean sPRIs (band 13 as the reference band) for two images (July 6, 2001 and August

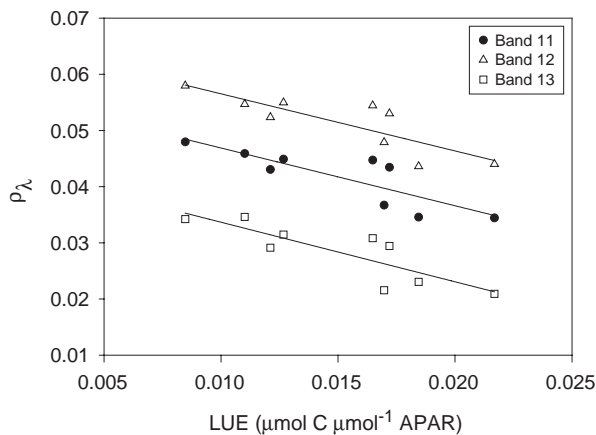


Fig. 8. Absolute surface reflectance (backscatter) from MODIS bands 11 (●), 12 (Δ), and 13 (□) versus LUE from tower data, for clear days during the growing seasons of 2001 to 2003 at the study site.

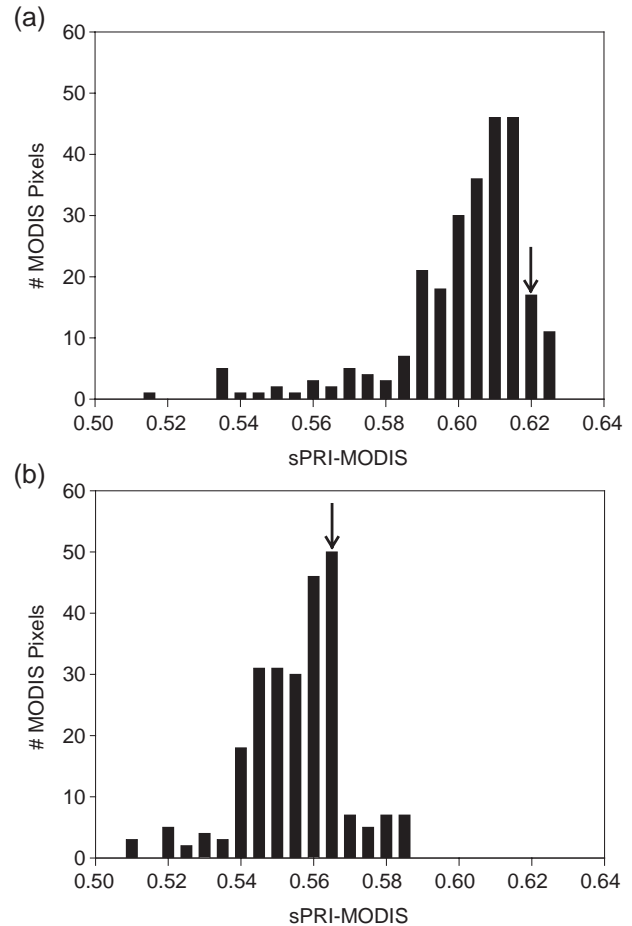


Fig. 9. Histograms of atmospherically corrected sPRI values for (a) July 6, 2001 and (b) August 14, 2003 for a regional analysis of all pixels classified as deciduous broadleaf forest within a 9904 km² area surrounding the Old Aspen flux tower in Saskatchewan, Canada. Arrows point to the classes where sPRIs from the flux tower are located. Number of pixels were 260 and 249 for 2001 and 2003, respectively.

14, 2003) having backscatter reflectance and large differences in LUE and sPRI for the tower site (circled data points in Fig. 7) showed a significant difference between the sPRIs in 2001 and 2003 ($P < 0.0001$). For the atmospherically corrected sPRIs, the means were 0.60 and 0.55 for 2001 and 2003, respectively (Fig. 9). For the atmospherically uncorrected dataset, the means were 0.65 and 0.62 for 2001 and 2003, respectively (not shown). In both cases (with and without atmospheric correction), the results were consistent with what we had found in the regression analysis of the tower data (Fig. 7).

4. Discussion

4.1. Variability in LUE and timing of MODIS overpasses

The original objective of this study was to use a MODIS-derived sPRI to observe physiology-related variations in photosynthetic LUE that occur at shorter temporal scales

(e.g., hourly, daily) than variations due to the canopy structural changes that can be detected using either ground-based measurements (e.g., phenology, LAI) (Chen, 1996; Chen & Cihlar, 1995; Huemmrich et al., 1999) or space-borne sensors (e.g., Chen & Cihlar, 1996; Goward et al., 1991; Huete et al., 2002; Justice et al., 1985; Kang et al., 2003). It is possible to obtain as many as four images per day from the sensors on Terra and Aqua so that it was plausible that within-day variations could be detected. The first difficulty that arose in using optical remote sensing data from space was the small range in LUE that was possible to be observed “from above” at the mid-day times of the MODIS overpasses compared to the full diurnal range in tower-measured LUE. We found great variability in LUE with increasing APAR levels when all growing-season days were considered. The variability in LUE and its magnitude were greatly reduced when clear days coincident with useful MODIS acquisitions were isolated (Fig. 4). These clear days generally corresponded to higher air temperatures and vapor pressure deficits and thus to low LUEs (Fig. 5). However, this narrow range in LUE at the time of our mid-day MODIS overpasses compared well with ranges in LUE observed in other PRI studies (e.g., Gamon et al., 1992; Nichol et al., 2000; Peñuelas et al., 1995, 1997).

A second factor limiting the range in detectable LUE was the timing of Terra and Aqua overpasses. The orbits of these two platforms were designed to allow the acquisition of morning and afternoon images over a same target at the equator (Barnes et al., 1998, 2002). However, since the current study was at a much higher latitude, the time window available for the analysis of the relationship between MODIS-derived sPRIs and tower-derived LUEs using either platform overpasses was compressed into a two-and-a-half hour period extending from 11:55 to 14:25 PM. In general, for any clear day, the magnitude and variations in LUE inside the observation period between noon and 14:00 were very small, thus diminishing the possibility to detect hourly variations in LUE from MODIS and, to a lesser extent, daily variations in LUE.

4.2. Regression analysis between LUE and sPRI

PRI is sensitive to variations in sun/sensor geometry, LAI, leaf angle distribution (LAD), atmospheric conditions, and background (Barton & North, 2001). Thus, even on the very homogenous site used in this study, we did not expect to find a relationship between sPRI, using either reference band, and LUE when all MODIS observations were included. Rahman et al. (2004), however, did find such a relationship using all views. We observed a larger range of sPRIs when using red bands (bands 1 or 13) as reference bands compared to using green reference bands (4 or 12) when all MODIS observations were included (see Fig. 6). This difference in sPRI ranges results from larger variations in the red band reflectances, compared to the green band, which could be due to changes in canopy structural and/or

optical properties (discussed below). It should be noted that MODIS does not have the 570 nm waveband usually used as the reference band in other PRI studies (e.g., Gamon et al., 1997; Peñuelas et al., 1995, 1997; Rahman et al., 2001; Trotter et al., 2002). Bands 4 and 12, the MODIS wavebands closest to 570 nm, are centered at 555 and 551 nm, respectively, although band 4 has a much wider bandwidth.

The photochemical mechanism that gives rise to a decrease in leaf reflectance at 531 nm with high light stress depends on the amount of APAR. Thus, a given canopy LUE will have different sPRIs depending on the amount of illuminated leaves seen by the sensor and the degree of illumination that occurs (Barton & North, 2001). Consequently, we expected to find an improved sPRI:LUE relationship when constraining the observations to pre-determined sun and sensor geometries (i.e., forward scatter versus backscatter or “near hot spot” observations). When using forward scatter data, none of the sPRIs tested in this study showed a correlation with LUE, neither for top-of-atmosphere or surface reflectance (see Fig. 7a for sPRI:LUE using reference band 13). This could be explained by the varying fractions of shadowed and sunlit canopy and background in the forward scatter direction. For a fixed LAI, LAD, and clear atmospheric conditions, the heterogeneity in sun/sensor geometry between MODIS observations will yield different sPRIs values without changes occurring in canopy LUE (Barton & North, 2001), thus contributing to the degradation of the sPRI:LUE relationship when forward scatter data are used.

When isolating reflectance data coming from the backscatter direction, the relationship between sPRI using band 13 as the reference band and LUE improved dramatically (Fig. 7b). It also improved to a lesser degree when band 12 was used as the reference band (data not shown). When viewed from the backscatter direction, the sensor sees a larger fraction of sunlit canopy. Thus, it is for these geometrical conditions that we are more likely to observe a consistent sPRI signal between scenes (i.e., approximately the same amount of sunlit leaves contributing to the total reflectance). In this study, sensor zenith angles varied between 30° and 40° for backscatter views. Since the target was viewed from angles close to nadir, the fraction of background elements and shadows contributing to the signal was higher than would be ideal to maximize views of canopy foliage.

From Fig. 7b, the highest LUEs and sPRIs occurred in 2001, while both 2002 and 2003 had lower values. These lower LUE and sPRI values correspond to lower measured total LAI values for 2002 and 2003 (3.99 and 4.03, respectively) compared to LAI in 2001 (5.22) (Barr et al., 2004). Barr et al. (2004) also reported lower GEP values for 2002–2003 compared to 2001. These low LAI and GEP values in 2002–2003 were due to the extended drought period that occurred between 2001 and 2003 in the study region (Agriculture & Agri-Food Canada, 2005; National

Climatic Data Center, 2005). Consequently, although we selected the aspen site for its uniform canopy, there are reasons to believe that the 2002 and 2003 drought resulted in larger canopy gap fractions and possibly increased contributions to the sPRI of background elements such as aspen bark (Kharouk et al., 1995) and hazelnut (*Corylus cornuta* Marsh.) understory, compared to 2001.

An increase in background contributions to the sPRI in 2002 and 2003 could have influenced sPRI in two ways. First, the hazelnut understory is a shade-adapted species. It has been shown that pools of xanthophyll cycle pigments in shade-adapted leaves are smaller than in sun-adapted leaves and that the de-epoxidation of violaxanthin to antheraxanthin and zeaxanthin poorly tracks LUE in shade-adapted leaves (Demmig-Adams & Adams, 1994; Thayer & Björkman, 1990). Consequently, when a significant fraction of the reflectance at 531 nm comes from a shade-adapted species, it would be expected that the sPRI–LUE relationship will be weakened. However, recent research on mature shade leaves of tropical species has shown that they can acclimate to prolonged direct light exposure by increasing their antheraxanthin and zeaxanthin levels (Krause et al., 2004).

The second plausible consequence of an increased contribution from the background reflectance in the backscatter direction due to a decrease in LAI could be a decrease in overall canopy chlorophyll content or the ratio of carotenoids to chlorophyll *a* (Filella et al., 2004). Since bands 11 and 12 are very close to one another, they are more likely to change in the same way in response to variations in canopy chlorophyll content. Band 13 contains a strong chlorophyll absorption feature compared to bands 11 and 12 and would therefore be expected to be more sensitive to changes in per-pixel chlorophyll content between 2002–2003 and 2001. Moreover, since 2002 and 2003 were the second and third years of the drought, low soil moisture conditions could also have affected the sPRI:LUE relationship.

Gamon et al. (1992) found a weak relationship between LUE of a water-stressed canopy and PRIs when using a narrow green band (550 nm) as the reference band. They also found better correlations between LUE and PRI for a water-stressed canopy when using longer reference wavelengths. In the latter case, however, PRI also showed a correlation with NDVI, indicating effects of the canopy structural changes on PRI. More recently, work by Sims et al. (in press) showed that the PRI:LUE relationship of chaparral species breaks down under extreme drought conditions. This reinforces our belief that extended dry conditions in the study area could have enhanced the effects of confounding structural factors in the sPRI signal and that these effects were more obvious when using band 13 as the reference band.

4.3. Change in absolute reflectance versus LUE

To investigate whether the differences in sPRIs between 2002–2003 and 2001 were due to changes in the

xanthophyll cycle pigments associated with photosynthetic down-regulation, or whether they were caused by indirect effects of low LAI values, or both, relationships between absolute reflectance (ρ_λ) in bands 11, 12, and 13, and LUE were analyzed. When plotted against LUE, the backscattered absolute surface reflectance in the three bands decreased with increasing LUE (Fig. 8). Although absolute reflectance at 531 nm was shown to be poorly correlated with LUE (Nichol et al., 2000), we still expected to observe an increase in reflectance with increasing LUE (Gamon et al., 1992; Peñuelas et al., 1995, 1997). As discussed in the previous section, large inter-annual variations in the canopy chlorophyll content relative to the small decrease in the reflectance at 531 nm due to physiological stress around midday can confound the physiological interpretation of the sPRI:LUE relationship when using backscattered observations. The higher slope of the ρ_{13} :LUE relationship, although not significantly different than the slopes for bands 11 and 12, reinforces the idea that variations in canopy chlorophyll content confounded the sPRI signal in the sPRI:LUE relationship, at least when using band 13 as the reference band and backscatter observations. Although our results suggest a possibility to remotely detect long-term variations in LUE at a coarse spatial scale, future research will be needed to assess the individual contributions of these factors on the sPRI signal and how they interact. Furthermore, the fact that the LUE versus sPRI relationship was conducted only for a single site places obvious limitations on our ability to make general inferences.

4.4. Atmospheric correction

It is of interest to note that the atmospheric correction, although increasing the goodness-of-fit of the ρ :LUE relationships for individual bands 11, 12, and 13 (Fig. 8), had opposite effects on the sPRI:LUE relationships when using reference bands 12 (data not shown) and 13 (Fig. 7). This was particularly noteworthy for sPRI using band 12, for which the sPRI:LUE relationship changed from a significant linear relationship ($r^2=0.52$, $P<0.03$) to an insignificant one ($r^2=0.15$, $P<0.3$) after atmospheric correction was applied. When using band 13 as the reference band, the sPRI:LUE relationship was better before ($r^2=0.76$) than after the atmospheric correction ($r^2=0.53$). At this point, we cannot say to what extent these differences between surface and top-of-atmosphere sPRIs are due to the MODIS-derived AOT values or to the model assumptions in 6S (e.g., Lambertian surface, continental model). Further analyses on this subject will involve the use of local aerosol measurements by sunphotometers.

4.5. Regional-scale comparison of sPRI

The drought that occurred between 2001 and 2003 allowed an examination of the regional stress response using MODIS-derived sPRIs. For two days from 2001 and

2003, distributions of MODIS sPRI for aspen-dominated pixels were created. Comparisons of the distributions suggest that sPRIs calculated for the tower pixel for these two dates were within the range of sPRIs for other deciduous pixels in a larger area (Fig. 9). Distribution histograms for the two dates are quite similar but the 2003 histogram is shifted towards lower sPRI values. This is in agreement with our finding of lower LUEs and sPRIs for 2003 compared to 2001, suggesting the possibility to remotely detect inter-annual variations in the LUE of other deciduous stands across large areas. On the other hand, given the other factors to which the PRI signal is sensitive at this spatial scale (e.g., stand structure, sun/sensor geometry), a physiological interpretation for the difference in mean sPRIs between these two years remains unclear.

5. Conclusions

We found a strong correlation between a MODIS-sPRI, calculated using surface reflectances from bands 11 (531 nm) and 13 (667 nm), and flux tower-derived photosynthetic light use efficiency (LUE) of a boreal aspen stand. However, this relationship was robust only when MODIS scenes with backscatter reflectance were used to calculate sPRI. This test of our ability to measure ecosystem-level light use efficiency of boreal deciduous forests from space was limited by the small ranges and magnitudes of tower LUE values on the clear days when useful MODIS acquisitions could be obtained. Furthermore, the orbital parameters of the Terra and Aqua satellites restricted MODIS acquisitions to a 2.5-h period in early afternoon at our study site when LUE values were typically lower than they were earlier in the day. At the spatial resolution of a MODIS pixel (1 km²), several factors appeared to confound the sPRI signal at 531 nm (e.g., sun/sensor geometry, background, atmosphere, canopy chlorophyll content) even for this homogeneous forest stand. Physiological interpretations of a MODIS-sPRI:LUE relationship using reference band 13 must be drawn with care, since the study was conducted only on a single site and because canopy structural and biochemical changes over time may both be involved in the reflectance signal. While PRI theory suggests that 531 nm reflectance should decrease with decreased LUE, we found increased reflectance not only at the 531 nm band, but at 551 nm, and 667 nm bands as well. All three of these bands are influenced by chlorophyll absorption.

In this study, we did not use the 570 nm reference band that has previously been employed for calculating PRI because MODIS does not have such a waveband. As an alternative, we used MODIS bands 12 and 13 since they were the closest narrow bands to 570 nm. Future satellites that include narrow wavebands at 531 and 570 nm might be better able to track short time-scale variations in LUE at regional to global scales, especially if their orbits were

planned to acquire scenes over a wider morning/afternoon time window. Furthermore, satellite-based hyperspectral sensors would allow more in-depth investigations of LUE using physiologically based vegetation indices since such a sensor could potentially discriminate between changes in xanthophylls, carotenoids, chlorophyll, and forest structure. Finally, tower-based hyperspectral measurements linked with space-based remote sensing are key to understanding the sPRI signal and its relationship with LUE of forest canopies so that such an approach can eventually be applied operationally in algorithms of ecosystem productivity.

Acknowledgments

We thank the Natural Sciences and Engineering Research Council of Canada (NSERC) and the Canadian Forest Service for the M.Sc. graduate fellowship and fellowship supplement provided to G. G. Drolet. We gratefully acknowledge support provided to the Fluxnet-Canada Research Network and Boreal Ecosystem Research and Monitoring Study (BERMS) by Canadian funding sources (NSERC, CFCAS, BIOCAP, Meteorological Service of Canada, Action Plan 2000, PERD). The NASA/GSFC contribution to this study was supported by an award to E. M. Middleton through the NASA Carbon Cycle Science Program. We thank Nazmi El Saleous for his technical support and Robert Knox and André Beaudoin for useful input along the way. H. Margolis gratefully acknowledges sabbatical support from the GEST Center of the University of Maryland, Baltimore County and the NASA Terrestrial Ecology Program.

References

- Agriculture and Agri-Food Canada. (2005). Drought watch [online]. Available from [accessed 7 April 2005].
- Amiro, B.D., Barr, A.G., Black, T.A., Iwashita, H., Kljun, N., McCaughey, J.H., Morgenstern, K., Murayama, S., Nesic, Z., Orchansky, A. L., Saigusa, N. (in press). Carbon, energy and water fluxes at mature and disturbed forest sites, Saskatchewan, Canada. *Agricultural and Forest Meteorology*.
- Baldocchi, D. (2003). Assessing the eddy covariance technique for evaluating carbon dioxide exchange rates of ecosystems: Past, present and future. *Global Change Biology*, 9, 479–492.
- Baldocchi, D. D., Hicks, B. B., & Meyers, T. P. (1988). Measuring biosphere–atmosphere exchanges of biologically related gases with micrometeorological methods. *Ecology*, 69, 1331–1340.
- Barnes, W. L., Pagano, T. S., & Salomonson, V. V. (1998). Prelaunch characteristics of the Moderate Resolution Imaging Spectroradiometer (MODIS) on EOS-AM1. *IEEE Transactions on Geoscience and Remote Sensing*, 4, 1088–1100.
- Barnes, W. L., Xiong, X., & Salomonson, V. V. (2002). Status of Terra MODIS and Aqua MODIS. *Proceedings of IGARSS 2002*, 2, Toronto, Canada, June 24–28 (pp. 970–972).
- Barr, A., Kljun, N., & Black, A. (2003). *Fluxnet-Canada methodology for estimating annual NEP: Filling gaps in NEP and obtaining R and GEP from NEP measurements using a moving window*

- Technique. Internal Fluxnet-Canada Research Network document, version 1.0.* 17 pages.
- Barr, A. G., Black, T. A., Hogg, E. H., Kljun, N., Morgenstern, K., & Nesic, Z. (2004). The seasonal cycle of leaf area index above a boreal aspen–hazelnut forest in relation to net ecosystem productivity. *Agricultural and Forest Meteorology*, 126, 237–255.
- Barton, C. V. M., & North, P. R. J. (2001). Remote sensing of light use efficiency using the photochemical reflectance index: Model and sensitivity analysis. *Remote Sensing of Environment*, 78, 264–273.
- Blanken, P. D., Black, T. A., Neumann, H. H., den Hartog, G., Yang, P. C., Nesic, Z., et al. (2001). The seasonal water and energy exchange above and within a boreal aspen forest. *Journal of Hydrology*, 245, 118–136.
- Blanken, P. D., Black, T. A., Yang, P. C., Neumann, H. H., Nesic, Z., Staebler, R., et al. (1997). Energy balance and canopy conductance of a boreal aspen forest: Partitioning overstory and understory components. *Journal of Geophysical Research*, 102(D24), 28915–28927.
- Bolin, B., & Fung, I. (1992). Report: The carbon cycle revisited. In D. Ojima (Ed.), *Modeling the earth system*. Boulder, Colorado, USA: UCAR/OIES (University Corporation of Atmospheric Research/Office of Inter-Disciplinary Earth Sciences).
- Chen, J. M. (1996). Optically-based methods for measuring seasonal variations of leaf area index in boreal conifer stands. *Agricultural and Forest Meteorology*, 80, 135–163.
- Chen, J. M., & Cihlar, J. (1995). Plant canopy gap size analysis theory for improving optical measurements of leaf area index. *Applied Optics*, 34, 6211–6222.
- Chen, J. M., & Cihlar, J. (1996). Retrieving leaf area index of boreal conifer forests using Landsat TM images. *Remote Sensing of Environment*, 55, 153–162.
- Chen, J. M., & Cihlar, J. (1998). *BOREAS RSS-07 LAI, gap fraction, and fPAR data. Data set*. Available online [<http://www.daac.ornl.gov>] from Oak Ridge National Laboratory Distributed Active Archive Center, Oak Ridge, Tennessee, U.S.A.
- Cramer, W., Bondeau, A., Woodward, F. I., Prentice, I. C., Betts, R. A., Brovkin, V., et al. (2001). Global response of terrestrial ecosystem structure and function to CO₂ and climate change: Results from six dynamic global vegetation models. *Global Change Biology*, 7, 357–373.
- Demmig-Adams, B., & Adams III, W. W. (1994). Capacity for energy dissipation in the pigment bed in leaves with different xanthophyll cycle pools. *Australian Journal of Plant Physiology*, 21, 575–588.
- Demmig-Adams, B., & Adams III, W. W. (1996). The role of xanthophylls cycle carotenoids in the protection of photosynthesis. *Trends in Plant Science*, 1, 21–26.
- Demmig-Adams, B., Moeller, D. L., Logan, B. A., & Adams III, W. W. (1998). Positive correlation between levels of retained zeaxanthin+antheraxanthin and degree of photoinhibition in shade leaves of *Schefflera arboricola* (Hayata) Merrill. *Planta*, 205, 367–374.
- Filella, I., Peñuelas, J., Llorens, L., & Estiarte, M. (2004). Reflectance assessment of seasonal and annual changes in biomass and CO₂ uptake of a Mediterranean shrubland submitted to experimental warming and drought. *Remote Sensing of Environment*, 90, 308–318.
- Gamon, J. A., Field, C. B., Bilger, W., Björkman, O., Freeden, A., & Peñuelas, J. (1990). Remote sensing of the xanthophyll cycle and chlorophyll fluorescence in sunflower leaves and canopies. *Oecologia*, 85, 1–7.
- Gamon, J. A., Peñuelas, J., & Field, C. B. (1992). A narrow-waveband spectral index that tracks diurnal changes in photosynthetic efficiency. *Remote Sensing of Environment*, 41, 35–44.
- Gamon, J. A., Serrano, L., & Surfus, J. S. (1997). The photochemical reflectance index: An optical indicator of photosynthetic radiation use efficiency across species, functional types, and nutrient levels. *Oecologia*, 112, 492–501.
- Goetz, S. J., & Prince, S. D. (1996). Remote sensing of net primary production in boreal forest stands. *Agricultural and Forest Meteorology*, 78, 149–179.
- Goetz, S. J., & Prince, S. D. (1998). Variability in carbon exchange and light utilization among boreal forest stands: Implications for remote sensing of net primary production. *Canadian Journal of Forest Research*, 28, 375–389.
- Goulden, M. L., Daube, B. C., Fan, S.-M., Sutton, D. J., Bazzaz, A., Munger, J. W., et al. (1997). Physiological responses of a black spruce forest to weather. *Journal of Geophysical Research*, 102(D24), 28987–28996.
- Goulden, M. L., Wofsy, S. C., Harden, J. W., Trumbore, S. E., Crill, P. M., Gower, S. T., et al. (1998). Sensitivity of boreal forest carbon balance to soil thaw. *Science*, 279, 214–217.
- Goward, S. N., Markham, B., Dye, D. G., Dulaney, W., & Yang, J. (1991). Normalized difference vegetation index measurements from the advanced very high resolution radiometer. *Remote Sensing of Environment*, 35, 257–277.
- Hall, F. G., Betts, A. K., Frohling, S., Brown, R., Chen, J. M., Chen, W., et al. (2004). The boreal climate. In P. Kabat, M. Claussen, P. A. Dirmeyer, J. H. C. Gash, L. B. Deguenni, M. Meybeck, R. A. Pielke, Sr., C. J. Vörösmarty, R. W. A. Hutjes, & S. Lütkeemeier (Eds.), *Vegetation, water, humans and the climate: A new perspective on an interactive system. Global Change IGBP Series* (pp. 93–114). Berlin: Springer-Verlag.
- Hall, F. G., & Knapp, D. (1999). *BOREAS TE-18 Landsat TM physical classification image of the SSA. Data set*. Available online [<http://www.daac.ornl.gov>] from Oak Ridge National Laboratory Distributed Active Archive Center, Oak Ridge, Tennessee, U.S.A.
- Heinsch, F. A., Reeves, M., Bowker, C. F., Votava, P., Kang, S., Milesi, C., et al. (2003). *User's Guide: GPP and NPP (MOD17A2/A3) Products. NASA MODIS Land Algorithm. Version 2.0*. Available online at: <http://www.ntsg.umd.edu/modis/MOD17UsersGuide.pdf>
- Hogg, E. H., Black, T. A., Neumann, H. H., Zimmermann, R., Hurdle, P. A., Blanken, P. D., et al. (1997). A comparison of sap flow and eddy fluxes of water vapor from a boreal deciduous forest. *Journal of Geophysical Research*, 102(D24), 28929–28938.
- Hogg, E. H., Brandt, J. P., & Kochtubajda, B. (2005). Factors affecting interannual variation in growth of western Canadian aspen forests during 1951–2000. *Canadian Journal of Forest Research*, 35, 610–622.
- Holt, N. E., Zigmantas, D., Valkunas, L., Li, X. P., Niyogi, K. K., & Fleming, G. R. (2005). Carotenoid cation formation and the regulation of photosynthetic light harvesting. *Science*, 307, 433–436.
- Huemmerich, K. F., Black, T. A., Jarvis, P. G., McCaughey, J. H., & Hall, F. G. (1999). High temporal resolution NDVI phenology from micro-meteorological radiation sensors. *Journal of Geophysical Research*, 104(D22), 27935–27944.
- Huete, A., Didan, K., Miura, T., Rodriguez, E. P., Gao, X., & Ferreira, L. G. (2002). Overview of the radiometric and biophysical performance of the MODIS vegetation indices. *Remote Sensing of Environment*, 83, 195–213.
- Justice, C. O., Townshend, J. R. G., Holben, B. N., & Tucker, C. J. (1985). Analysis of the phenology of global vegetation using meteorological satellite data. *International Journal of Remote Sensing*, 6, 1271–1381.
- Kattenberg, A., Giorgi, F., Grassl, H., Mitchell, G. A., Meehl, J. F. B., Stouffer, R. J., et al. (1996). Climate models — projections of future climate. In J. T. Houghton, L. G. Meira Filho, B. A. Callender, N. Harris, A. Kattenburg, & K. Maskell (Eds.), *Climate change 1995 — the science of climate change*. New York, USA: Cambridge University Press.
- Kang, S., Running, S. W., Lim, J.-H., Zhao, M., Park, C.-R., & Loehman, R. (2003). A regional phenology model for detecting onset of greenness in temperate mixed forests, Korea: An application of MODIS leaf area index. *Remote Sensing of Environment*, 86, 232–242.
- Kharouk, V. I., Middleton, E. M., Spencer, S. L., Rock, B. N., & Williams, D. L. (1995). Aspen bark photosynthesis and its significance to remote sensing and carbon budget estimates in the boreal ecosystem. *Water, Air and Soil Pollution*, 82, 483–497.

- Krause, G. H., Grube, E., Koroleva, O. Y., Barth, C., & Winter, K. (2004). Do mature shade leaves of tropical tree seedlings acclimate to high sunlight and UV radiation? *Functional Plant Biology*, 31, 743–756.
- Martel, M.-C., Margolis, H. A., Coursolle, C., Bigras, F. J., Heinsch, F. A., & Running, S. W. (2005). Decreasing photosynthesis at different spatial scales during the late growing season on a boreal cutover. *Tree Physiology*, 25, 689–699.
- Middleton, E., & Sullivan, J. (2000). *BOREAS TE-10 leaf optical properties for SSA species. Data set*. Available online [http://www.daac.ornl.gov] from Oak Ridge National Laboratory Distributed Active Archive Center, Oak Ridge, Tennessee, U.S.A.
- Mitchell, J. F. B., Manabe, S., Meleshko, V., & Tokioka, T. (1990). Equilibrium climate change and its implications for the future. *Climate change: The 1990 scientific assessment*. New York: Cambridge University Press.
- Monteith, J. L. (1972). Solar radiation and productivity in tropical ecosystems. *Journal of Applied Ecology*, 9, 747–766.
- Monteith, J. L. (1977). Climate and the efficiency of crop production in Britain. *Philosophical Transactions of the Royal Society of London. Series B*, 281, 277–294.
- Myneni, R., Hoffman, Y., Knyazikhin, et al. (2002). Global products of vegetation leaf area and fraction absorbed PAR from one year of MODIS data. *Remote Sensing of Environment*, 76, 139–155.
- National Climatic Data Center (2005). *North American drought monitor [online]*. Available from <http://www.ncdc.noaa.gov/oa/climate/monitoring/drought/nadm/> [accessed 7 April 2005].
- Nichol, C. J., Huemmrich, K. F., Black, T. A., Jarvis, P. G., Walthall, C. L., Grace, J., et al. (2000). Remote sensing of photosynthetic-light-use efficiency of boreal forest. *Agricultural and Forest Meteorology*, 101, 131–142.
- Peñuelas, J., Fillela, I., & Gamon, J. (1995). Assessment of photosynthetic radiation-use efficiency with spectral reflectance. *New Phytologist*, 131, 291–296.
- Peñuelas, J., Llusia, J., Piñol, J., & Fillela, I. (1997). Photochemical reflectance index and leaf photosynthetic radiation-use efficiency assessment in Mediterranean trees. *International Journal of Remote Sensing*, 18, 2863–2868.
- Rahman, A. F., Cordova, V. D., Gamon, J. A., Schmid, H. P., & Sims, D. A. (2004). Potential of MODIS ocean bands for estimating CO₂ flux from terrestrial vegetation: A novel approach. *Geophysical Research Letters*, 31, L10503.
- Rahman, A. F., Gamon, J. A., Fuentes, D. A., Roberts, D. A., & Prentiss, D. (2001). Modeling spatially distributed ecosystem flux of boreal forest using hyperspectral indices from AVIRIS imagery. *Journal of Geophysical Research*, 106(D24), 33579–33591.
- Running, S. W., Baldocchi, D. D., Turner, D. P., Bakwin, P. S., & Hibbard, K. A. (1999). A global terrestrial monitoring network integrating tower fluxes, flask sampling, ecosystem modeling and EOS satellite data. *Remote Sensing of Environment*, 70, 108–128.
- Running, S. W., Nemani, R. R., Heinsch, F. A., Zhao, M., Reeves, M., & Hashimoto, H. (2004). A continuous satellite-derived measure of global terrestrial primary production. *Bioscience*, 54, 547–560.
- Running, S. W., Thornton, P. E., Nemani, R. R., & Glassy, J. M. (2000). Global terrestrial gross and net primary productivity from the earth observing system. In O. Sala, R. Jackson, & H. Mooney (Eds.), *Methods in ecosystem science* (pp. 44–57). New York: Springer-Verlag.
- SAS Institute (2000). *SAS/STAT user's guide, vol. 1* (4th ed.). Cary, SC, USA: SAS Institute.
- Schlesinger, W. H. (1997). *Biogeochemistry: An analysis of global change*. (2nd ed.). San Diego, CA: Academic Press.
- Sellers, P. J., Hall, F. G., Kelly, R. D., Black, T. A., Baldocchi, D. D., Berry, J. A., et al. (1997). BOREAS in 1997: Experiment overview, scientific results, and future directions. *Journal of Geophysical Research*, 102, 28731–28769.
- Sellers, P. J., Hall, F. G., Margolis, H. A., Kelly, R., Baldocchi, D., den Hartog, J., et al. (1995). Boreal Ecosystem-Atmosphere Study (BOREAS): An overview and early results from the 1994 field year. *Bulletin of the American Meteorological Society*, 76, 1549–1577.
- Sims, D. A., Luo, H., Hastings, S., Oechel, W. C., Rahman, A. F., Gamon, J. A. (in press). Parallel adjustments in vegetation greenness and ecosystem CO₂ exchange in response to drought in a Southern California chaparral ecosystem. *Remote Sensing of Environment*.
- Thayer, S. S., & Björkman, O. (1990). Leaf xanthophyll content and composition in sun and shade determined by HPLC. *Photosynthesis Research*, 23, 331–343.
- Trotter, G. M., Whitehead, D., & Pinkney, E. J. (2002). The photochemical reflectance index as a measure of photosynthetic light use efficiency for plants with varying foliar nitrogen contents. *International Journal of Remote Sensing*, 23, 1207–1212.
- Turner, D. P., Ollinger, S. V., & Kimball, J. S. (2004). Integrating remote sensing and ecosystem process models for landscape- and regional-scale analysis of the carbon cycle. *Bioscience*, 54, 573–584.
- Turner, D. P., Ritts, W. D., Cohen, W. B., Gower, S. T., Zhao, M., Running, S. W., et al. (2003). Scaling Gross Primary Production (GPP) over boreal and deciduous forest landscapes in support of MODIS GPP product validation. *Remote Sensing of Environment*, 88, 256–270.
- Turner, D. P., Urbanski, S., Bremer, D., Wofsy, S. C., Meyers, T., Gower, S. W., et al. (2003). A cross-biome comparison of daily light use efficiency for gross primary production. *Global Change Biology*, 9, 383–395.
- Vermote, E. F., Tanre, D., Deuze, J. L., Herman, M., & Morcrette, J. J. (1997). Second simulation of the satellite signal in the solar spectrum, 6S: An overview. *IEEE Transactions on Geoscience and Remote Sensing*, 35(3), 675–686.
- Yamamoto, H. Y. (1979). Biochemistry of the violaxanthin cycle in higher plants. *Pure Applied Chemistry*, 51, 639–648.